Tunability of free-electron lasers

R. K. Wong and W. B. Colson
Physics Department, Naval Postgraduate School, Monterey, California 93943
(Received 11 October 1994)

In a free-electron laser oscillator, a variation in the electron beam energy leads to a change in the resonant optical frequency. Simulations are used to study the optical response to an electron beam energy change. A step change in the electron beam energy is used to define a characteristic response time for changing the optical frequency.

PACS number(s): 41.60.Cr

In a free-electron laser (FEL), a relativistic electron beam oscillates as it travels through a spatially periodic magnetic undulator. The electron beam oscillations create and amplify light whose wavelength is determined by the electron beam energy and undulator field structure. The optical frequency can be tuned by adjusting the energy of the electron beam. In a FEL oscillator, the optical pulse evolves through mode competition as a result of losses at the mirrors and wavelength dependent amplification by the electron beam. The characteristic time observed for the wavelength change determines the optical response to an electron beam energy change.

The ability of the FEL to change the optical frequency rapidly has been demonstrated experimentally [1] and theoretically [2,3]. Of similar interest is the ability to stabilize the optical frequency through feedback [4] where the optical frequency is monitored and fluctuations are corrected through a feedback loop that adjusts the electron energy accordingly. Experimental work focusing on wavelength shifting has also been performed where the results were related to a simple analytical model [5]. For FEL applications, it is important to understand the nature of the time response and how the FEL changes its frequency.

Simulations use FEL theory based on a self-consistent solution to the coupled Maxwell-Lorentz equations [6] describing the evolution of the optical pulse in a FEL oscillator over many passes [7]. Transverse effects are neglected to focus on the more important longitudinal behavior. The simulations examine the characteristic time scale of the optical response as a function of the gain, resonator loss, electron pulse length, desynchronism, and electron beam energy shift.

I. FEL THEORY WITH DIMENSIONLESS PARAMETERS

A self-consistent FEL theory couples single-particle electron dynamics following the Lorentz force equations with a wave equation derived from Maxwell's equations [6]. Dimensionless parameters [7] can be used to simplify the description of the interaction between the electron beam and the optical wave. A carrier wavelength λ with a slowly varying complex amplitude and phase represents the optical field. The interaction is assumed to be near resonance where an electron passes through one period of the undulator as one wavelength of light passes over the electron. The interaction with the optical field causes bunching of the electrons in the longitudinal direction which is necessary to coherently amplify the optical wave. The electron phase $\zeta=(k+k_0)z-\omega t$ can be defined to follow the microscopic longitudinal evolution of an electron relative to the optical wave, where z is oriented along the propagation direction, $\omega=2\pi c/\lambda$ is the optical frequency, $k=2\pi/\lambda$, $k_0=2\pi/\lambda_0$, λ_0 is the undulator wavelength, and c is the speed of light. The corresponding electron phase velocity is given by

$$\nu=\frac{d\zeta}{d\tau}=L[(k+k_0)\beta_z-k]\ , \tag{1}$$

for electrons with velocity $\beta_z c$ in the z direction in an undulator with N periods and length $L=N\lambda_0$. The dimensionless time $\tau=ct/L$ is measured from $\tau=0$ at the beginning of the undulator to $\tau=1$ at the end of the undulator. Within the optical field envelope, longitudinal distances are normalized to the "slippage length" $N\lambda$, the distance that an electron traveling at speed $\beta_z c$ falls behind light traveling at speed c during one pass through the undulator [7]. The equations of motion for an electron can be reduced to the pendulum equation [8]

$$\frac{d^2\zeta_{z+\tau}}{d\tau^2}=|a_z|\cos(\zeta_{z+\tau}+\phi_z)\ , \tag{2}$$

following electron phases at position $z+\tau$ in the presence of the complex dimensionless optical field $a=4\pi NeK[J_0(\xi)-J_1(\xi)]LEe^{i\phi}/\gamma^2 mc^2$ where e is the electron charge magnitude, $\gamma=(1-\beta_\perp^2-\beta_z^2)^{-1/2}$ is the relativistic Lorentz factor, $\beta_\perp c$ is the transverse electron velocity, and ϕ is the optical phase. The optical field in (2), $|a_z|e^{i\phi_z}$, is evaluated at position z. The subscript $z+\tau$ accounts for the slippage of the electron pulse as it falls behind the optical field, $a_z=|a_z|e^{i\phi_z}$, at position z. The Bessel functions J_0 and J_1, with argument $\xi=K^2[2(1+K^2)]$, describe the reduced coupling in a linearly polarized undulator [9]. The undulator parameter is $K=e\bar{B}\lambda_0/2\pi mc^2$ where $\bar{B}$ is the root-mean-squared undulator field strength and m is the electron mass. Us-

ing Maxwell's wave equation and the slowly varying amplitude and phase approximation, the evolution of the complex optical field amplitude is described by [7]

$$\frac{\partial a_z}{\partial \tau} = -\langle je^{-i\zeta} \rangle_{z+\tau} , \tag{3}$$

where the dimensionless current density is $j = 8N\{e\pi K[J_0(\xi) - J_1(\xi)]L\}^2 \rho F/\gamma^3 mc^2$ and ρ is the electron beam particle density. The transverse coupling is described by the filling factor $F = \pi r_b^2/\pi w_0^2$ where r_b is the electron beam radius and w_0 is the optical mode radius [7]. The average $\langle\ \rangle$ over the individual sample electrons determines their contribution to the current density driving the optical wave. The longitudinal macroscopic electron pulse profile is assumed to be parabolic, $j(z) = j_0(1 - 2z^2/\sigma_z^2)$, with pulse length σ_z and peak current j_0. The macroscopic electron pulse shape $j(z)$ typically does not change due to microscopic bunching.

In the simulations, the optical wave and electron beam are represented by a large number of sites along the longitudinal z axis. Each electron site contains electrons uniformly distributed in phase at the start of each pass. As the electrons slip back through the slippage distance $N\lambda$, the coupled equations (2) and (3) are solved numerically.

At the beginning of each pass, the dimensionless desynchronism d, normalized to the slippage distance $N\lambda$, is added to shift the optical pulse with respect to the electron pulse. A small value of desynchronism is necessary for the development of a steady-state optical pulse [7]. On each pass, the optical pulse requires a finite time to bunch the electrons. As the bunched electrons slip back across the optical pulse each pass, they preferentially amplify its trailing edge and distort the optical pulse. Over many passes, this distortion causes the optical pulse centroid to move back away from the electrons and decay. The loss per pass is given by the resonator quality factor Q, so that the optical field decays as $|a|^2 \propto \exp(-n/Q)$ when the gain is zero [7].

The electron phase velocity v describes changes in either the optical wavelength or the electron beam energy. At resonance, $v = 0$, the optical wavelength is determined by the resonance condition $\lambda = \lambda_0(1 - \beta_z) \approx \lambda_0(1 + K^2)/\gamma^2$ when $\gamma \gg 1$. From (1) and holding λ constant, a change in the electron beam energy by $\Delta\gamma mc^2$ away from resonance results in a phase velocity change of $\Delta v = 4\pi N \Delta\gamma/\gamma$. Therefore, a change in electron phase velocity Δv is directly proportional to a small change in electron beam energy.

The phase velocity also can be used to measure changes in the optical wavelength. The optical spectrum is comprised of a large number of modes, each mode represented by a phase velocity, $v(k) = L[(k + k_0)\beta_z - k]$, where $k = 2\pi/\lambda$ is the mode wave number. A change of Δk, or $\Delta\lambda$, results in a change in the phase velocity of $\Delta v = -2\pi N \Delta k/k = 2\pi N \Delta\lambda/\lambda$, so that a small change in v is directly proportional to a small change optical wavelength λ. In order for the FEL to maintain resonance, a shift in Δv in the initial electron phase velocity due to a change of initial electron energy leads to a shift of $-\Delta v$ in the optical spectrum.

II. OPTICAL PULSE EVOLUTION

Figure 1 shows the evolution of the longitudinal optical pulse shape and power spectrum resulting from a simulation. The parameters $j_0 = 1$, $Q = 50$, $\sigma_z = 2$, and $d = 0.03$ are chosen so that the optical pulse reaches steady-state saturation at field strengths that do not lead to the trapped-particle instability and the growth of optical sidebands [10]. Across the top three frames of Fig. 1, the steady-state optical pulse is shown after $n = 500$ passes. The sequence of four rows of frames below this set shows the evolution at increments of 50 passes after a step change of the electron phase velocity by $\Delta v_0 = \pi/2$. The shift of $|\Delta v_0| = \pi/2$ in this simulation is within the gain bandwidth of a normal FEL. The left frames display the optical pulse amplitude $|a(z)|$ as a function of the dimensionless longitudinal position z. The peak value of the dimensionless field is $|a| = 13$ at 500 passes, and the frames below are in the same scale as the top frame. The bottom left frame shows the relative position of the electron pulse slipping back across the optical pulse from the beginning of the undulator ($\tau = 0$) in black to the end of the undulator ($\tau = 1$) in grey. The desynchronism value of $d = 0.03$ results in the optical pulse arriving ahead of the electron pulse at each pass. The loss due to a finite $Q = 50$ provides for an exponentially decaying profile along the leading edge of the optical pulse where there is no gain. The step change in initial phase velocity modulates the pulse structure in the interaction region. After 550 passes, a small amplitude rise due to this modulation begins to travel across the longitudinal profile due to desynchronism d each pass. A separation occurs between the light at the initial frequency in front of this rise and the light of a new frequency behind it.

The center frames display the evolution of the optical power spectrum $P(v,n)$. The horizontal axis for the optical spectrum is directly proportional to a change in wavelength according to $\Delta v = 2\pi N \Delta\lambda/\lambda$. A triangular grey marker on the bottom of each frame marks the new shifted electron phase velocity at the beginning of each pass. The electron beam energy is initially at resonance, $v_0 = 0$,

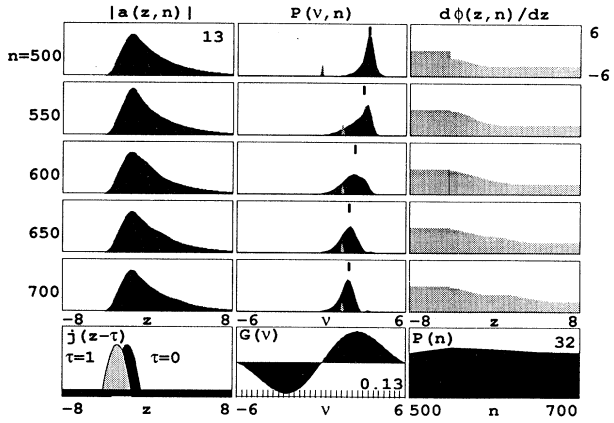

FIG. 1. Optical pulse evolution for $j_0 = 1, Q = 50$, $d = 0.03$, and $\sigma_z = 2$ following a step change in the electron energy.

at the beginning of each pass up to pass $n=500$. The centroid of the optical spectrum is represented by a rectangular black marker at the top of each frame. The optical spectrum centered initially on resonance at the beginning of the simulation, $n=0$, has shifted in the steady state to $\nu(k)\approx 3$ through mode competition and saturation prior to pass $n=500$ [6]. The weak field gain spectrum $G(\nu)$ is shown below the optical spectra for reference and can be used to explain this shift. The gain spectrum shows that at resonance net single-mode gain does not occur, while a shift of the electron energy off resonance with optical wave of $\nu_0=2.6$ results in peak single-mode gain $G=0.135j=0.135$ for weak fields ($|a|\ll\pi$). In strong fields at saturation, the peak gain moves to higher values of ν and determines the location of the observed steady state of the optical spectrum at pass $n=500$. The change in electron beam energy $\Delta\gamma mc^2$ corresponds to a shift in phase velocity $\Delta\nu=4\pi N\Delta\gamma/\gamma$. The optical spectrum centroid indicated by the rectangular marker at the top of the frame begins to shift to the left toward smaller wavelengths as the spectrum broadens at $n=550$ passes. A well-defined peak develops at the new frequency after $n=650$ passes and grows to its steady-state value by 700 passes. For $\Delta\nu=1.5$ there is a fractional decrease of the optical wavelength $\Delta\lambda/\lambda=\Delta\nu/2\pi N\approx 0.25\%$ after $n=500$ passes for $N=100$. The increase in initial electron beam energy leads to a decrease in optical wavelength.

The right frames represent the change in the slope of the optical phase, $d\phi/dz$, along the longitudinal pulse position. The variation of the optical phase ϕ describes frequency components around the carrier wavelength λ. An optical wave with dependence of the form $\exp[i(kz-\omega t+\phi)]$ has an effective wave number modifying the phase velocity, $k\rightarrow k+d\phi/dz$. The change from the initial phase velocity ν_0 is $\Delta\nu=-d\phi/dz$. To the left of the electron pulse, the optical phase slope has its original value $d\phi/dz=0$. To the right of the electron pulse at 500 passes, the slope is $d\phi/dz\approx -3$, representing the change in the optical phases that shifts the optical frequency from its initial value to reach steady state. The change in the shape of the complex optical field envelope determines the wavelength shift, from the fundamental carrier wavelength. In the interaction region, $d\phi/dz$ is not constant and gives a frequency chirp to the optical spectrum. The plot of $d\phi/dz$ shows an increase in the optical frequency from the back to the front of the pulse. After $n=550$ passes, $d\phi/dz$ has increased in the region of interaction. After $n=600$ passes, the new frequency begins to grow to the left of the electron pulse and follows the motion of the rise in the field magnitude $|a(z)|$.

The power $P(n)=|a(n)|^2$ integrated over the length of the pulse is shown in the lower right plot. The power increases when the width of the optical spectrum broadens at 550 passes and then returns to its steady-state value. This is a result of the choice of operating parameters. Other parameters can lead to a decrease in power.

Figure 2(a) shows the response in the centroid of the optical spectrum to the electron energy step in the stimulation of Fig. 1. The vertical axis is the absolute value of $\Delta\nu$ measuring changes in both the phase velocity of the electrons and the centroid of the optical spectrum. The shape of the curve is approximately an exponential rise of the form $\Delta\nu\propto 1-e^{-(n-n_0)/n_c}$, where n_0 is the pass number at which the energy step is applied and n_c is the characteristic number of passes for the optical spectrum centroid to reach $1/e$ of the new steady-state value. For a sudden energy step, the characteristic response times is $n_c=90$. The time for light of the initial frequency to decay is on the order of Q, or about 50 passes, and is in rough agreement with n_c. The shape of the response is not greatly affected by the amplitude and sign of the electron energy shift for values in this range and these operating parameters. For a larger energy shift where the electrons move outside the gain bandwidth, the shape of the response is strongly dependent on both the amplitude and sign of the electron beam energy shift [2]. In this case, the initial fields decay away completely and the new fields grow from spontaneous emission.

Figure 2(b) shows the response to a linear energy slew of the electron beam over $n_s=200$ passes for the same operating parameters as in Fig. 2(a). The slope of the energy slew is less than the slope of the response in Fig. 2(a). The optical response is driven by the more gradual change in $\Delta\nu_0$. The slope of the energy slew and the opti-

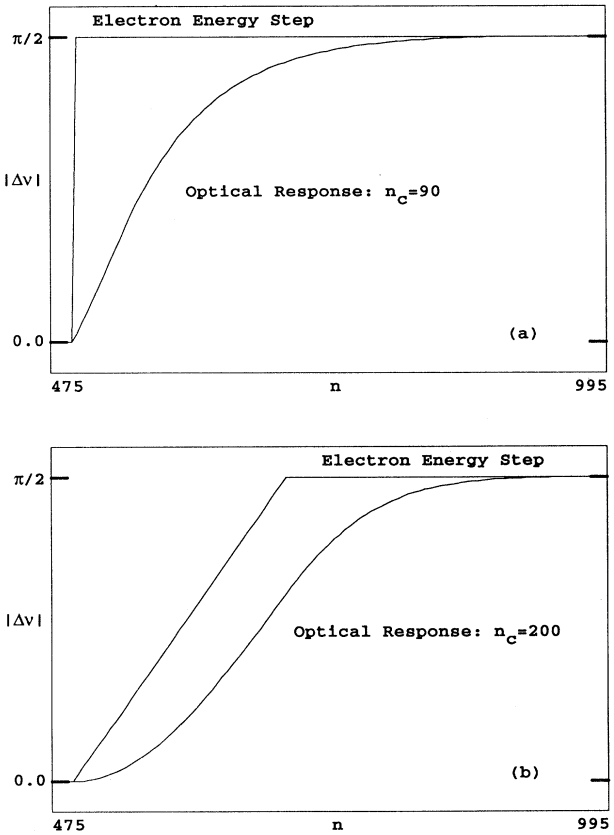

FIG. 2. (a) Response of the optical centroid to a step change in the electron energy, $n_s=0$, with $j_0=1$, $Q=50$, $d=0.03$, and $\sigma_z=2$. (b) Response of the optical centroid to an energy slew over $n_s=200$ passes with $j_0=1$, $Q=50$, $d=0.03$, and $\sigma_z=2$.

cal response are equal at the center of the phase velocity change. The response of the optical centroid occurs over a period characterized by $n_c \approx 200$ passes. The initial optical response is slower in Fig. 2(a) since the energy shift is more gradual.

Figure 3 shows the results of a simulation with the same parameters of the previous figures, but with a higher value of $Q=150$. The higher Q requires a longer time for the optical pulse to reach steady state, so the energy shift in this simulation occurs after $n=1000$ passes. Outside the region of interaction with the electron pulse, the optical pulse extends over a longer distance due to the effects of desynchronism and lower resonator loss. Note that the simulation window width in the longitudinal direction is twice that in the previous simulation. The maximum amplitude $|a(z)|=16$ is larger than in Fig. 1 and the longer optical pulse results in a narrower optical linewidth for $P(\nu,n)$. A distinct "bump" is evident in the longitudinal optical pulse shape where the energy shift occurs. With large Q, light of the initial frequency does not decay until about 400 passes after the step in initial electron energy. The bump that represents the transition from the initial to the final optical frequencies is a small portion of the total optical energy leading to two distinct peaks in the optical spectrum at $n=1200$ passes. While the initial peak, which decays with Q, greatly influences the optical pulse centroid, the peak at the final frequency grows to a significant value in about 100 passes less than determined by Q. Light is generated at the final frequency in less time than determined by Q. From the evolution of $d\phi/dz$, it is apparent that by $n=1100$ passes the field within the interaction region is at the final frequency.

In Fig. 4 the evolution of the optical pulse is shown for peak current $j_0=0.4$, $Q=40$, desynchronism $d=0.01$, and for a larger electron pulse length of $\sigma_z=5$. A change in phase velocity $\Delta\nu=\pi/2$ is imposed after $n=1000$ passes. Outside the region of interaction with the electron pulse, the optical pulse decays rapidly for low Q. In comparison with the two previous figures, the low Q results in a narrower pulse despite a larger σ_z resulting in a wider optical spectrum $P(\nu,n)$. The slope of the optical

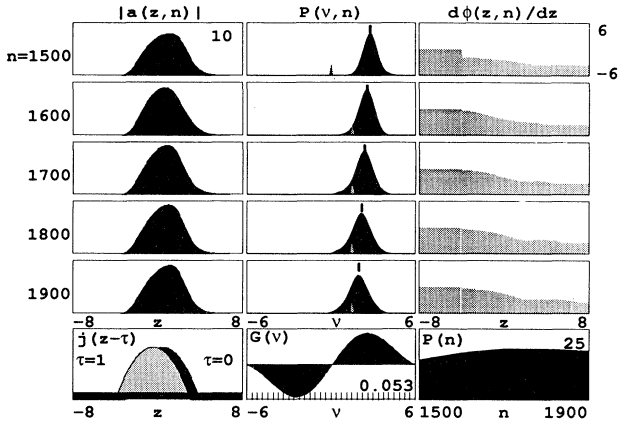

FIG. 4. Optical pulse evolution for $j_0=0.4$ and $\sigma_z=5$ with small $Q=40$ and small desynchronism $d=0.01$.

phase shows higher frequencies at the front part of the pulse and lower frequencies in the rear part of the pulse, as in the previous example. The front of the pulse has reached the steady pulse shape after 30 passes. The desynchronism d determines the rate at which optical information is transferred to the front of the optical pulse. The time for optical information to be transferred is $\sigma_z/d \approx 500$ passes, and the optical pulse shape and optical centroid reach a steady state on this same time scale.

III. TRENDS IN THE OPTICAL RESPONSE

In Fig. 5, the response is plotted for the simulation of Fig. 4. Even for a small value of $Q=40$, the characteristic number of passes in $n_c \approx 450$. In the middle portion of the frequency shift, the optical centroid changes linearly with the number of passes. The time scale to reach the new steady-state frequency is on the order of $\sigma_z/d \approx 500$. This is the time that information takes to travel across the optical pulse $|a(z)|$ due to the desynchronism process.

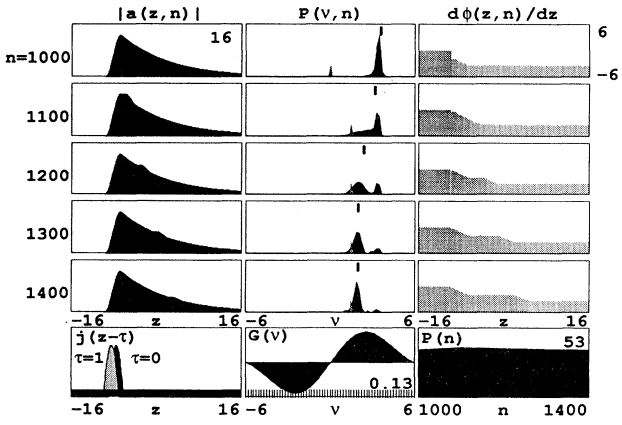

FIG. 3. Optical pulse evolution for $j_0=1$, $d=0.03$, and $\sigma_z=2$ with large resonator $Q=150$.

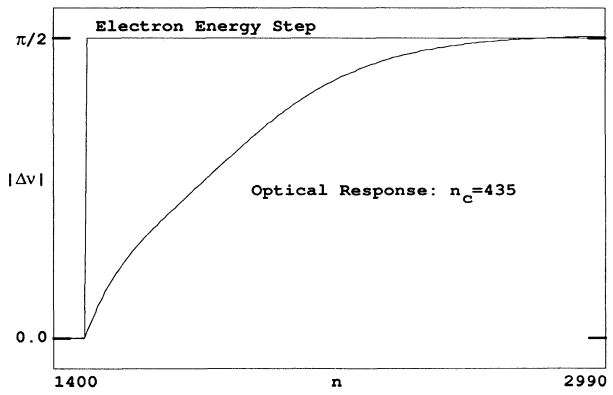

FIG. 5. Response of the optical centroid to a step change in the electron energy, $n_s=0$, from Fig. 4 with $j_0=0.4$, $Q=40$, $d=0.01$, and $\sigma_z=5$.

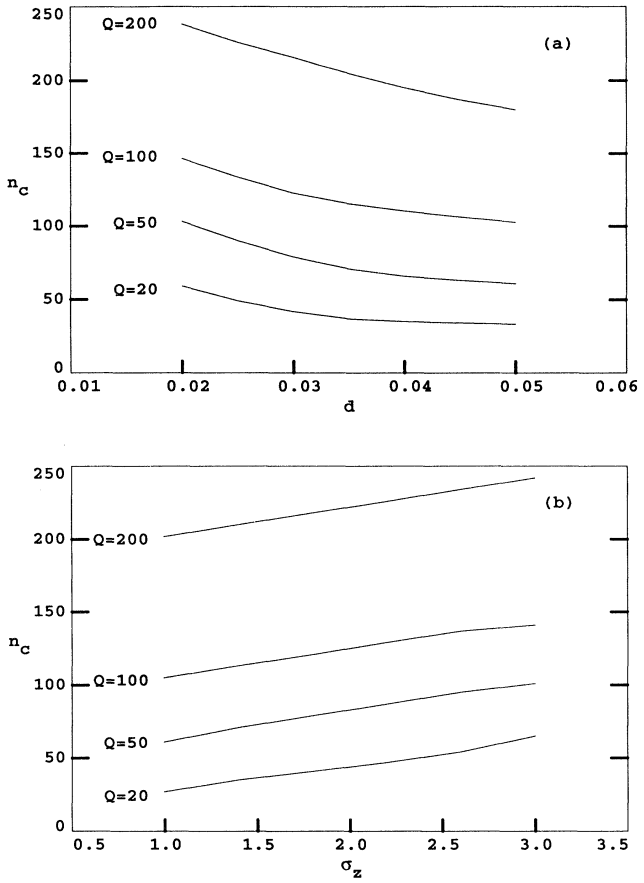

FIG. 6. (a) Characteristic response time n_c as a function of desynchronism d with $j_0=1.0$ and $\sigma_z=1.8$. (b) Characteristic response time n_c as a function of pulse length σ_z with $j_0\sigma_z=1.8$ and $d=0.03$.

The actual time to reach equilibrium is a function of the FEL operating parameters. For pulses with $\sigma_z/d > Q$, increases in current j and decreases in Q are found to lower the value of n_c. For low Q the larger σ_z/d, the characteristic response time is dependent on the sign of the shift in the electron phase velocity.

The optical response time is studied by following the centroid of the optical spectrum for different values of Q, d, σ_z, j, and energy step. In Fig. 6(a), the desynchronism is varied from $d=0.01$ to 0.06 for a family of curves with $Q=20$, 50, 100, and 200. The decay time n_c approaches Q for $d\approx 0.03$. For large Q and small σ_z/d, the response is governed by the decay of light at the old frequency outside the interaction region. For small $Q \leq 50$, the transit time σ_z/d is comparable to the decay time. For a given value of Q, n_c is inversely proportional to σ_z. The range of the curves displayed have been set so that fields remain weak where the trapped-particle instability and limit-cycle behavior do not occur. For $j_0=1.0$ and $\sigma_z=1.8$, the optical pulse overlap results in strong coupling for values of $d \leq 0.02$ and $Q > 100$. Values of $d \geq 0.05$ results in weak coupling for lower values of Q, and the pulse decays so that no steady state is reached.

In Fig. 6(b), the electron pulse length σ_z is varied holding the product $j_0\sigma_z=1.8$ fixed. This holds the total charge in the electron pulse constant. The desynchronism is chosen to be $d=0.03$. A family of curves is again plotted for the same range of Q as in Fig. 6(a). For a small value of σ_z, the characteristic number of passes n_c is approximately equal to Q. As the value of σ_z increases, the time that the modulation travels across the electron pulse is on the order of σ_z/d. The increase in n_c with σ_z/d is within a factor of two of this argument. For fixed Q, n_c is observed to increase linearly with σ_z.

IV. SUMMARY

The FEL oscillator has been studied using simulations that follow the evolution of the optical pulse over many passes. The response of the optical frequency to a change in the initial electron beam energy depends strongly on the resonator quality factor Q and the time σ_z/d for information exchange over the optical pulse. The resonator Q determines the optical response time due to the decay outside the interaction region. Within the interaction region, the characteristic number of passes required to shift to a new frequency is approximately σ_z/d. For small Q, σ_z/d is the predominate factor in the optical response. Even for large Q, σ_z/d determines the rate at which light will be generated at the new frequency. These characteristics compare well to previous experimental work [5] of the FEL wavelength shifting process.

[1] R. W. Swent, K. W. Berryman, H. A. Schwettman, and T.I. Smith, Nucl. Instrum. Methods A **304**, 272 (1991).
[2] W. Wilkenson, Master's thesis, Naval Postgraduate School, 1993 (unpublished).
[3] G. Shvets and J. Wurtele, Physics of Plasmas, No. 1, (1994) 157.
[4] A. Marziali and T. I. Smith, Nucl. Instrum. Methods A **331**, 59 (1993).
[5] A. Marziali, Ph.D. dissertation, Stanford University, 1994 (unpublished).
[6] W. B. Colson and S. K. Ride, Phys. Lett A **76**, 379 (1980).
[7] W. B. Colson, *Free Electron Laser Handbook,* edited by W. B. Colson, C. Pellegrini, and A. Renieri (North-Holland, Amsterdam, 1990), Chap. 5.
[8] W. B. Colson, Ph.D. dissertation, Stanford University, 1977 (unpublished).
[9] W. B. Colson, IEEE J. Quantum Electron. **Q-17**, 1417 (1990).
[10] W. B. Colson, Nucl. Instrum. Methods A **250**, 168 (1986).